Published in final edited form as:
Sci Signal. ; 6(261): ra8. doi:10.1126/scisignal.2003638.

Mitochondrial Reactive Oxygen Species Promote Epidermal Differentiation and Hair Follicle Development

Robert B. Hamanaka[1], **Andrea Glasauer**[1], **Paul Hoover**[2], **Shuangni Yang**[2], **Hanz Blatt**[2], **Andrew R. Mullen**[3], **Spiro Getsios**[2], **Cara J. Gottardi**[1], **Ralph J. DeBerardinis**[3], **Robert M. Lavker**[2], and **Navdeep S. Chandel**[1,*]

[1]Department of Medicine, The Feinberg School of Medicine, Northwestern University, Chicago, IL 60611, USA.

[2]Department of Dermatology, The Feinberg School of Medicine, Northwestern University, Chicago, IL 60611, USA.

[3]Department of Pediatrics, University of Texas Southwestern Medical Center at Dallas, Dallas, TX 75390, USA.

Abstract

Proper regulation of keratinocyte differentiation within the epidermis and follicular epithelium is essential for maintenance of epidermal barrier function and hair growth. The signaling intermediates that regulate the morphological and genetic changes associated with epidermal and follicular differentiation remain poorly understood. We tested the hypothesis that reactive oxygen species (ROS) generated by mitochondria are an important regulator of epidermal differentiation by generating mice with a keratinocyte-specific deficiency in mitochondrial transcription factor A (TFAM), which is required for the transcription of mitochondrial genes encoding electron transport chain subunits. Ablation of TFAM in keratinocytes impaired epidermal differentiation and hair follicle growth and resulted in death 2 weeks after birth. TFAM-deficient keratinocytes failed to generate mitochondria-derived ROS, a deficiency that prevented the transmission of Notch and β-catenin signals essential for epidermal differentiation and hair follicle development, respectively. In vitro keratinocyte differentiation was inhibited in the presence of antioxidants, and the decreased differentiation marker abundance in TFAM-deficient keratinocytes was partly

*To whom correspondence should be addressed. nav@northwestern.edu.

SUPPLEMENTARY MATERIALS

www.sciencesignaling.org/cgi/content/full/6/261/ra8/DC1

Fig. S1. Analysis of epidermal apoptosis and epidermal thickness in control and *TFAM* cKO skin.
Fig. S2. Sensitivity of control keratinocyte differentiation to exogenous H_2O_2 and inhibition of mitochondrial calcium uptake.
Fig. S3. Analysis of cellular signaling pathways in control and *TFAM* cKO keratinocytes.
Fig. S4. Sensitivity of Notch signaling to ROS during keratinocyte differentiation.
Fig. S5. Sensitivity of Wnt–β-catenin signaling to ROS in epidermal keratinocytes.

Author contributions: R.B.H. and N.S.C. designed the study, analyzed the data, and wrote the manuscript. R.B.H., S.G., C.J.G., R.M.L., and N.S.C. collaborated on experimental design. R.B.H. and A.G. carried out the experiments. S.Y. and H.B. assisted with histology. P.H. assisted with cell isolation and organotypic raft cultures. A.R.M. and R.J.D. performed the metabolic labeling experiments. All authors discussed the results and commented on the manuscript.

Competing interests: The authors declare that they have no competing interests. The content is solely the responsibility of the authors and does not necessarily represent the official views of the NIH.

rescued by application of exogenous hydrogen peroxide. These findings indicate that mitochondria-generated ROS are critical mediators of cellular differentiation and tissue morphogenesis.

INTRODUCTION

The skin epidermis is a self-renewing stratified epithelium that serves as a barrier against external insults as well as excessive fluid loss. This epidermal barrier depends on a continual cycle in which cells in the proliferative basal layer exit the cell cycle and differentiate as they move outward through the suprabasal layers (1, 2). Factors that regulate the homeostatic renewal of the epidermis include Notch, p63, AP2, and CCAAT/enhancer-binding protein (C/EBP) transcription factors (3–5). Hair is maintained by a cycle in which hair follicles undergo periods of growth (anagen), regression (catagen), and rest (telogen) (6). During anagen, cells in the bulge region of the hair follicle give rise to the outer root sheath and the transit-amplifying cells of the hair follicle matrix, which differentiate into the inner root sheath and the hair shaft itself. In catagen, the cells of the outer root sheath and matrix undergo apoptosis and the hair follicle retracts (7, 8). Little is known, however, about the molecular signaling events that regulate differentiation within the epidermis or hair follicle.

Reactive oxygen species (ROS) have classically been thought of as cellular damaging agents that play a causal role in various human pathologies (9). However, evidence has accumulated to implicate ROS as critical regulators of cellular function and homeostasis. ROS serve as signaling intermediates in cellular signaling pathways, including those that regulate oxygen sensing, cellular proliferation, innate immunity, and adrenal steroidogenesis (10–14). We have demonstrated that the differentiation of human bone marrow–derived mesenchymal stem cells into adipocytes requires mitochondrial generation of ROS to activate differentiation-specific transcriptional programs, suggesting that ROS may play an early, causal role in cellular differentiation (15). Aberrantly increased cellular ROS content is associated with precocious differentiation of *Drosophila* hematopoietic stem cells and exhaustion of mammalian hematopoietic stem cells (16–18). Furthermore, cellular differentiation correlates with increases in mitochondrial mass and cellular ROS content in several systems (19–22). It is not known, however, whether mitochondrial ROS are required for cellular differentiation and tissue morphogenesis in vivo.

To test the hypothesis that mitochondria-derived ROS regulate cellular differentiation within the epidermis, we deleted the gene encoding mitochondrial transcription factor A (*TFAM*) in the epidermis of mice using Cre recombinase expressed under the control of the keratin 14 promoter (*KRT14-Cre*). TFAM is required for transcription and replication of the mitochondrial genome, which encodes critical subunits of the electron transport chain (23). Cells lacking TFAM cannot generate mitochondrial adenosine 5′-triphosphate (ATP) through oxidative phosphorylation or produce ROS (24, 25). Mice lacking TFAM in the epidermis exhibited impaired epidermal differentiation and hair development. The interfollicular epidermis of $TFAM^{fl/fl}/KRT14\text{-}Cre^{+}$ mice was characterized by reduced expression of differentiation-specific genes and by increased proliferation within the basal

layer. Primary keratinocytes isolated from *TFAM*$^{fl/fl}$/*KRT14-Cre*$^{+}$ mice showed reduced differentiation in vitro as a result of impaired Notch-dependent transcription. Exogenous hydrogen peroxide (H_2O_2) rescued the expression of differentiation markers, whereas differentiation of control primary keratinocytes was inhibited by treatment with antioxidants. Further, the hair follicles of *TFAM*$^{fl/fl}$/*KRT14-Cre*$^{+}$ mice underwent premature catagen and exhibited reduced abundance of β-catenin, a result of impaired Wnt signaling in the absence of mitochondrial ROS. Together, our results demonstrate that the generation of mitochondrial ROS is a key upstream signaling event required for the development and homeostasis of the epidermis and hair follicle.

RESULTS

TFAM$^{fl/fl}$/*KRT14-Cre*$^{+}$ mice, hereinafter referred to as *TFAM* conditional knockout (cKO) mice, were born in the expected Mendelian ratios and were remarkable by postnatal day 3 (P3) for their lack of hair (Fig. 1A). The epidermis of *TFAM* cKO mice lacked TFAM and mitochondrial-encoded proteins, such as Cox1 (cytochrome *c* oxidase subunit 1), but maintained nuclear-encoded mitochondrial proteins, such as NDUFS3 [NADH (reduced form of nicotinamide adenine dinucleotide) dehydrogenase (ubiquinone) iron-sulfur protein 3] and SDHA (succinate dehydrogenase subunit A) (Fig. 1B). Histological analysis of the dorsal skin of TFAM-deficient mice at P3 revealed a normal epidermis with reduced amounts of subcutaneous fat compared to that of control mice (*TFAM*$^{fl/fl}$*; KRT14 Cre*$^{-}$) (Fig. 1C). By P6, the hair follicles of *TFAM* cKO epidermis appeared to have prematurely entered catagen, which was confirmed by positive staining for cleaved caspase 3 (Fig. 1D). Cells positive for cleaved caspase 3 were confined to the hair follicles, and no increase in apoptosis was observed in the interfollicular epidermis (fig. S1A). *TFAM* cKO mice showed increased epidermal thickness at P9 (Fig. 1C and fig. S1, B and C). *TFAM* cKO mice stopped gaining weight and had a median survival of 13 days, likely because of an epidermal barrier defect (as assessed by toluidine blue exclusion) that developed in these mice (Fig. 1, E and F). Heterozygous *TFAM*$^{fl/+}$*; K14Cre*$^{+}$ mice were normal in appearance and had no survival defect.

The thicker epidermis and barrier defect observed in *TFAM* cKO mice led us to examine biochemical markers of epidermal differentiation in the skin of control and *TFAM* cKO mice. The abundance of keratin 10 (a marker of differentiated suprabasal keratinocytes) was reduced in *TFAM* cKO epidermis, whereas that of keratin 14 (a marker of undifferentiated basal cells) was increased (Fig. 2A). Immunohistochemistry (IHC) revealed reduced abundance of the terminal differentiation markers loricrin and involucrin in the epidermis of *TFAM* cKO mice (Fig. 2B). Keratin 14, which was confined to the basal layer of control epidermis, was also present in the suprabasal layers of *TFAM* cKO epidermis. Staining with Oil Red O revealed that TFAM cKO epidermis lacked mature sebaceous glands (Fig. 2C).

Epidermal basal cells must balance proliferation and differentiation to maintain epidermal homeostasis (1). To assess epidermal proliferation, P6 control and *TFAM* cKO mice were injected subcutaneously with 5-bromo-2′-deoxyuridine (BrdU), and the number of cells that had entered S phase of the cell cycle was determined. Proliferation within the basal keratinocyte layer of *TFAM* cKO epidermis was significantly increased compared with

control skin (Fig. 2, D and E). Collectively, these findings indicate that loss of mitochondrial function impairs epidermal differentiation, promoting maintenance of a basal, proliferative phenotype.

We next investigated the bioenergetic, ROS-generating, and biosynthetic capacity of the mitochondria of *TFAM* cKO keratinocytes. Primary keratinocytes isolated from *TFAM* cKO mice demonstrated significantly reduced oxygen consumption compared with control (Fig. 3A). *TFAM* cKO keratinocytes also displayed reduced amounts of cellular superoxide and H_2O_2 as measured by oxidation of hydroethidine and CM-H_2DCFDA, respectively (Fig. 3, B and C). These results indicate the impaired mitochondrial function of *TFAM* cKO keratinocytes. Cells with normally functioning mitochondria use intermediary metabolites of the citric acid cycle as biosynthetic precursors for the macromolecular synthesis required for proliferation (26). Because the basal keratinocyte layer of *TFAM* cKO epidermis exhibited increased proliferation (Fig. 2, D and E), we inquired about the paradoxical ability of these cells with impaired mitochondrial function to meet their biosynthetic needs. We have demonstrated that cancer cells that lack mitochondrial electron transport chain function can use glutamine-dependent reductive carboxylation to supply intermediates for biosynthesis (27). This process involves the reverse flux of glutamine-derived α-ketoglutarate through isocitrate dehydrogenases 1 and 2 to promote production of citrate, which is required for lipid synthesis. We thus cultured primary keratinocytes isolated from control and *TFAM* cKO mice in the presence of uniformly labeled [^{13}C]glutamine or [^{13}C]glucose and measured ^{13}C enrichment of cellular citrate by mass spectrometry. After labeling with [^{13}C]glucose, cellular citrate pools from *TFAM* cKO keratinocytes were enriched for unlabeled product (M+0), indicating reduced oxidative metabolism of glucose in *TFAM* cKO keratinocytes (Fig. 3D). Labeling with [^{13}C]glutamine revealed that *TFAM* cKO keratinocytes produced significantly more citrate with 5 additional mass units (M+5) than control keratinocytes, consistent with the activation of reductive carboxylation in these cells (Fig. 3E). These results suggest that primary *TFAM* cKO keratinocytes use alternative metabolic pathways to promote proliferation within the epidermis.

To more directly test the role that mitochondrial signaling plays in keratinocyte differentiation, we exploited the ability of primary keratinocytes to differentiate upon an increase in the concentration of extracellular calcium (“calcium switch”) (28). After calcium switch, *TFAM* cKO keratinocytes failed to increase the abundance of the terminal differentiation markers desmoglein 1, involucrin, and loricrin (Fig. 4A). Because *TFAM* loss impairs mitochondrial ATP production in addition to ROS production, we sought to determine whether treatment with exogenous H_2O_2 could rescue the ability of *TFAM* cKO keratinocytes to differentiate after calcium switch. *TFAM* cKO keratinocytes were cultured in the presence of calcium, with a combination of galactose and the galactose-metabolizing enzyme galactose oxidase, which produces H_2O_2 in culture medium (29). Addition of galactose with galactose oxidase restored the accumulation of involucrin and loricrin in *TFAM* cKO keratinocytes in a dose-dependent manner (Fig. 4B), suggesting that it is the lack of mitochondrial ROS production that prevents *TFAM* cKO keratinocytes from differentiating. Upon calcium switch plus galactose and galactose oxidase, control keratinocytes did not exhibit increased expression of differentiation markers, and at high

amounts of galactose oxidase, differentiation was inhibited, suggesting that cellular oxidants can promote differentiation over a narrow range of concentrations (fig. S2A).

To confirm further that mitochondrial ROS promote keratinocyte differentiation, we used mitochondria-targeted mito-vitamin E (MVE), an antioxidant that consists of vitamin E covalently coupled to a triphenylphosphonium (TPP) cation (30). Treatment of control keratinocytes with MVE, but not with TPP, inhibited the calcium-mediated induction of differentiation markers (Fig. 4C). Similar effects were observed in cells treated with the superoxide dismutase and catalasemimetic EUK134 (31) (Fig. 4D). Treatment of control keratinocytes with the mitochondrial calcium uptake inhibitor RU360 (32) inhibited the induction of differentiation markers after addition of calcium to culture media, suggesting that calcium uptake into mitochondria may be required for differentiation signaling (fig. S2B). Loss of TFAM did not inhibit signaling through the Akt or mitogen-activated protein kinase (MAPK) signaling pathways (fig. S3A). Phosphorylation of AMP-activated protein kinase (AMPK) was increased in*TFAM* cKO keratinocytes; however, phosphorylation of AMPK decreased in both cell lines after treatment with calcium (fig. S3B), suggesting that these pathways are properly regulated in the absence of TFAM. Collectively, these data indicate that mitochondria-generated ROS are required for the differentiation of primary keratinocytes in the presence of calcium.

To study the relevance of our findings to human epidermis, we used an organotypic raft model of human epidermis. This model consists of human foreskin keratinocytes grown on a collagen matrix at an air-medium interface, resulting in a stratified, differentiated three-dimensional culture that exhibits the major characteristics of native epidermis (33). When grown at an air-medium interface for 12 days, human keratinocytes grew into a stratified epithelium and showed increased abundance of epidermal differentiation markers; this was prevented by EUK134 treatment (Fig. 4, E and F). Collectively, our data indicate that mitochondrial ROS are required for human and mouse epidermal differentiation.

Activation of Notch signaling is required for keratinocyte differentiation both in vivo and after treatment of cultured primary keratinocytes with calcium (5, 34, 35). We observed decreased abundance of several Notch-regulated transcripts in epidermal lysates from P9 *TFAM* cKO mice compared with control mice, suggesting that Notch signaling is inhibited in the epidermis of these mice (Fig. 5A). Calcium switch led to the induction of a Notch/RBP-J (recombination signal binding protein for immunoglobulin κ J region) luciferase reporter as well as induction of the Notch target mRNAs *Hes1*, *Hey1*, and *Hey2* in control keratinocytes, a response that was abolished in *TFAM* cKO keratinocytes (Fig. 5B and fig. S4A). A similar suppression of Notch activation after calcium treatment was observed in control keratinocytes treated with MVE or EUK134 (fig. S4, B and C). This demonstrates the requirement for mitochondrial ROS generation in the transduction of Notch signals during keratinocyte differentiation. Consistent with keratinocytes that have impaired Notch activity, *TFAM* cKO keratinocytes did not show increased transcription of *KRT1* and *KRT10* mRNAs after calcium switch (Fig. 5C). However, expression of the active Notch intracellular domain (NICD) was sufficient to induce expression of *KRT1* and *KRT10* in both control and *TFAM* cKO cells, further suggesting that the lack of keratinocyte

differentiation observed in *TFAM* cKO cells is the result of impaired Notch signaling (Fig. 5D).

Previous studies have demonstrated that β-catenin–dependent transcription is essential for proper formation and homeostasis of hair follicles in vivo (36, 37). Hair follicles from conditional β-catenin knockout epidermis are characterized by early onset of first catagen in which the hair follicle epithelium separates from the dermal papilla, which is similar to our observations (Fig. 1C) (36). β-Catenin was decreased in abundance in P6 or P9 *TFAM* cKO hair follicles and showed less cytoplasmic and nuclear staining compared with control (Fig. 6A and fig. S5A).

To determine whether *TFAM* cKO cells can respond to Wnt ligand stimulation with β-catenin–dependent transcription, we treated *TFAM* cKO and control keratinocytes with control or Wnt3a-conditioned medium. Wnt3a-conditioned medium activated transcription of the β-catenin/TCF target gene *Axin2* in control but not in *TFAM* cKO keratinocytes. Similarly, infection of control keratinocytes with adenovirus encoding Wnt3a induced a T cell factor/lymphoid enhancer factor (TCF/LEF) responsive luciferase reporter in control but not in *TFAM* cKO keratinocytes (Fig. 6B). These results were recapitulated in control keratinocytes treated with either MVE or EUK134 (fig. S5, B and C). These observations suggest that the lack of hair follicle growth in the *TFAM* cKO mice was due to the inability to produce mitochondrial ROS, resulting in impaired Wnt–β-catenin transcriptional activation.

Although *TFAM* cKO keratinocytes show defective induction of β-catenin–dependent transcription downstream of Wnt stimulation, both sets of keratinocytes could induce gene expression upon treatment with lithium chloride (LiCl), which activates β-catenin–dependent transcription by inhibiting glycogen synthase kinase 3β (GSK-3β)–mediated degradation of β-catenin (Fig. 6C). This suggested to us that a ROS-dependent signaling event upstream of GSK-3β was deficient in *TFAM* cKO cells. Exogenous H_2O_2 can activate β-catenin through oxidation of the thioredoxin-like protein nucleoredoxin (NXN), which binds to and inhibits the upstream β-catenin activator Dishevelled (Dsh), an interaction that is inhibited by ROS-mediated oxidation of NXN (38). To test whether endogenous mitochondrial ROS were required for oxidation of NXN, control and *TFAM* cKO keratinocytes were infected with adenovirus encoding either Wnt3a or green fluorescent protein (GFP) as a control. When cellular lysates were resolved on a nonreducing polyacrylamide gel, two bands specific for NXN were observed: a slower-migrating band that corresponded to nonoxidized NXN and a faster-migrating band that corresponded to oxidized NXN (Fig. 6D). The oxidation of NXN was increased by Wnt3a in control but not in *TFAM* cKO keratinocytes, suggesting that mitochondrial ROS are required for oxidation of NXN after Wnt stimulation. LiCl treatment did not induce oxidation of NXN, consistent with LiCl acting directly on GSK-3β, downstream of NXN (Fig. 6E).

Because LiCl could rescue β-catenin–dependent transcription in *TFAM* cKO keratinocytes, we attempted to rescue the hair follicle defect observed in *TFAM* cKO mice by treating postpartum mice with LiCl. At P7, pups were sacrificed and skin sections were taken. Although LiCl did not completely rescue the hair growth defect of *TFAM* cKO mice,

treatment resulted in an increase in the length of hair follicles (Fig. 6F and fig. S5D), suggesting that the follicular defect observed in *TFAM* cKO mice is a result of defective β-catenin–dependent transcription.

DISCUSSION

Increased mitochondrial mass and cellular ROS content have been correlated with cellular differentiation in various systems (16–22); however, it is unknown whether this is simply a response to the metabolic demands of differentiation or whether mitochondrial signaling plays a primary role in this process. Using targeted deletion of *TFAM* in epidermal basal keratinocytes, we showed that mitochondrial retrograde signaling is a key upstream event in the keratinocyte differentiation program. *TFAM* cKO epidermis displayed several signs of inhibited differentiation, including reduced abundance of terminal differentiation markers and increased abundance of basal cell markers. Moreover, *TFAM* cKO epidermis was significantly more proliferative than control epidermis. Although a caveat to our approach is that *TFAM* cKO keratinocytes lacked production of mitochondrial ATP as well as of ROS, TFAM-deficient keratinocytes could meet the energetic demands for proliferation, and thus, it is likely that the impaired differentiation observed in *TFAM* cKO epidermis was a result of impaired cellular signaling pathways and not a result of energy depletion. We further demonstrated that *TFAM* cKO keratinocytes could meet the biosynthetic demands of proliferation through glutamine-dependent reductive carboxylation. Previous reports have demonstrated that cancer cells can use this alternative metabolic pathway to supply biosynthetic intermediates for proliferation (27, 39, 40). We demonstrated that primary nontransformed mammalian cells can also carry out this alternative metabolic pathway if the mitochondrial electron transport chain is compromised.

By isolating primary mouse keratinocytes from *TFAM* cKO mice, we were able to further corroborate our in vivo observations. Treatment with exogenous H_2O_2 restored the induction of keratinocyte differentiation markers in *TFAM* cKO keratinocytes, and through the use of mitochondria-targeted antioxidants, we demonstrated that mitochondrial ROS are required for keratinocyte differentiation in control keratinocytes that have an intact mitochondrial electron transport chain. Loss of mitochondrial ROS production impaired the Notch-dependent transcription required for keratinocyte differentiation, and expression of the Notch intracellular domain rescued *KRT1* and *KRT10* expression in *TFAM* cKO keratinocytes. It remains to be determined how ROS promote Notch activity during keratinocyte differentiation. We have identified the asparaginyl hydroxylase FIH1 [factor inhibiting HIF-1α (hypoxia-inducible factor-1α)] as a key inhibitor of Notch transcriptional activity and keratinocyte differentiation (41). The activity of FIH1 is inhibited by endogenous concentrations of H_2O_2, suggesting that a peroxide-FIH1-Notch signaling arm may regulate keratinocyte differentiation (42). Additionally, HIF-1α interacts with the Notch intracellular domain to promote transcription of target genes (43, 44). Mitochondrial ROS promote HIF-1α stabilization (45). Thus, it is possible that Notch-HIF interactions are disrupted because of diminished mitochondrial ROS production in *TFAM* cKO keratinocytes. Future experiments will be required to determine the precise mechanism by which mitochondrial ROS stimulate Notch activity.

High doses of exogenous H_2O_2 promote NXN oxidation and β-catenin–dependent transcription. We showed that endogenous, mitochondria-produced ROS are required for activation of β-catenin downstream of Wnt ligand stimulation. The inability of *TFAM* cKO keratinocytes to activate β-catenin is partially responsible for the lack of hair in *TFAM* cKO mice. This hair defect could be partially rescued with LiCl, which we demonstrated activates β-catenin downstream of mitochondrial ROS. Human mutations in mitochondrial DNA have been associated with skin and hair abnormalities (46). It will be of interest to examine whether disruption of mitochondria-dependent ROS signaling occurs in diseases associated with skin and hair abnormalities.

Baris and colleagues have also generated mice lacking TFAM in the epidermis (47), which die within the first week after birth. Although they show reduced abundance of loricrin and keratin 10 in the epidermis of their mice, Baris and colleagues conclude that epidermal differentiation occurs normally in *TFAM* cKO mice. The authors also report that *TFAM* cKO mice do not have an epidermal barrier defect; however, these experiments were done on neonatal mice. We observed that barrier integrity was lost as the mice aged (Fig. 1E). Although the $TFAM^{fl/fl}$ mice used in both studies are on a C57BL/6 background, the backgrounds of the *KRT14-Cre* mice differ [B6CBAF1 in the present study, C57BL/6 in (47)], which could contribute to the observed life span differences.

Previous studies have focused on the role that high concentrations of cellular ROS play in disrupting homeostasis (9, 48, 49). Increased concentrations of cellular ROS are associated with various human pathologies including cancer, diabetes, and neurodegeneration, leading to clinical trials involving high doses of antioxidants to target cellular oxidants in human disease. However, these trials have consistently been unsuccessful, and there is evidence that these treatments may even increase mortality (50–54). An important implication of our findings is that therapies involving high doses of antioxidants could impair mitochondrial retrograde signaling, preventing proper differentiation within progenitor cell populations.

MATERIALS AND METHODS

Mice and keratinocyte culture

$TFAM^{fl/fl}$ C57BL/6 mice were generated as previously described (25) and were crossed with *KRT14-Cre* B6CBAF1 mice purchased from The Jackson Laboratory (stock no. 004782). Heterozygous $TFAM^{fl/+};K14Cre^{+/-}$ mice were mated back to $TFAM^{fl/fl}$ to obtain control and *TFAM* cKO mice. To obtain primary mouse keratinocytes, pups were skinned at P1 or P2. Epidermis was separated from dermis by overnight incubation in dispase (5 mg/ml) and disrupted using TrypLE Select (Invitrogen). Cells were cultured in CnT07 medium (CELLnTEC) (0.07 mM $CaCl_2$) supplemented with uridine (100 μg/ml) and 1 mM sodium pyruvate. Calcium switches were performed in CnT02 medium (CELLnTEC) (1.2 mM $CaCl_2$) supplemented with uridine (100 μg/ml) and 1 mM sodium pyruvate. Mitochondria-targeted vitamin E and TPP control were used as antioxidants at 1 μM. EUK134 was used at 50 μM.

For human organotypic raft cultures, human epidermal keratinocyte cultures were prepared and grown as previously described (55). Cells were treated with DMSO or EUK134 on the day cells were transferred to the air-medium interface.

Lentiviral luciferase reporter constructs were purchased from SABiosciences. Wnt3a-conditioned medium for qRT-PCR experiments was produced from L-Wnt3a cells [American Type Culture Collection (ATCC) stock CRL-2647]. Control medium was produced from L cells (ATCC stock CRL-2648). For TCF/LEF luciferase reporter assay and NXN Western blots, control or *TFAM* cKO keratinocytes were infected with adenovirus expressing either Wnt3a or GFP as a control.

Mouse keratinocytes were treated with 10 mM LiCl or NaCl as a control for 16 hours. For NaCl and LiCl injections, postpartum mice received LiCl (200 mg/kg) or an equimolar dose of NaCl as control. Pups were sacrificed at P7, and skin was stained with H&E to detect hair follicles.

Histology and immunostaining

Excised dorsal epidermal tissues were fixed in 10% buffered formalin and embedded in paraffin. Four-micrometer sections were placed on charged slides. For automated IHC, slides were baked for 2 hours at 50°C and rehydrated through graded alcohols. Endogenous peroxidase was blocked for 10 min [H_2O_2 in methanol (MeOH)], and epitopes were retrieved in Citrate Retrieval Solution (NeoMarkers) for 1 hour at 95°C. IHC protein block (DAKO) and antibody diluents (DAKO) were used in accordance with the DAKO LV-1 Auto Stainer Plus system. The primary antibody dilutions used were as follows: loricrin (rabbit, 1:3000, Abcam), involucrin (rabbit, 1:4000, Abcam), keratin 10 (rabbit, 1:200, Covance), keratin 14 (rabbit, 1:500, Covance), and β-catenin (mouse, 1:200, Cell Marque). Slides were incubated with EnVision Dual-Link (rabbit/mouse, predilute, DAKO) followed by Liquid DAB+ (DAKO) and Mayer's hematoxylin (DAKO) counterstain before dehydration and coverslipping in Sub-X mounting medium. Imaging was performed with a Zeiss Axioplan 2 microscope and a high-resolution AxioCam digital color camera. Image analysis was performed with Zeiss AxioVision software.

For in vivo BrdU labeling experiments, P6 mice were injected subcutaneously with a single dose of BrdU (50 μg/g). After 1 hour, dorsal epidermis was collected and fixed as above. Anti-BrdU antibody (mouse, 1:2000, DAKO) was used to visualize proliferation index.

Oil Red O (0.5% in isopropanol) was diluted 3:2 in dH_2O and filtered. For detection of sebaceous glands using Oil Red O, frozen sections were fixed in 50%formalin, washed in H_2O, and rinsed in 60% isopropanol for 2 min. Sections were stained with Oil Red O solution for 15 min, rinsed with 60% isopropanol, and stained with hematoxylin.

For cleaved caspase 3 immunofluorescence, frozen sections were blocked in 10% serum followed by overnight incubation with primary antibody (Cell Signaling, 1:50). Goat anti-rabbit Alexa 555 (Invitrogen, 1:300) was used, followed by DAPI (4′,6-diamidino-2-phenylindole) staining (20 mg/ml) and mounting in Gelvatol mounting medium.

Western blots

Cells were lysed in Urea Sample Buffer [8 M deionized urea, 1% SDS, 10% glycerol, 60 mM tris (pH 6.8), 0.1% pyronin-Y, 5% β-mercaptoethanol] or Cell Lysis Buffer (Cell Signaling), and lysates were resolved on 4 to 20% Criterion gels (Bio-Rad) and transferred onto nitrocellulose. The antibodies used were Cox1 (Invitrogen), NDUFS3 (Mitosciences), SDHA (Mitosciences), TFAM (a gift from G. Shadel, Yale University), desmoglein 1 (clone 27B2, Santa Cruz Biotechnology), loricrin (Covance), involucrin (mouse, Covance; human, Sigma), keratin 10 (mouse, Covance; human, Santa Cruz Biotechnology), keratin 14 (Covance), actin (Sigma), nucleoredoxin (Proteintech), GAPDH (glyceraldehyde-3-phosphate dehydrogenase), pSer^{473} Akt, Akt, phospho–extracellular signal–regulated kinase 1/2 (pERK1/2), ERK1/2, phospho–mitogen-activated or extracellular signal–regulated protein kinase kinase (pMEK), MEK, pAMPK, and AMPK (Cell Signaling). Blots were quantified with ImageJ software.

qRT-PCR

Total RNA was extracted from cells with TRIzol reagent (Invitrogen), and 1 μg was reverse-transcribed with RETROscript first strand synthesis kit (Ambion). qRT-PCR was performed on a Bio-Rad iCycler iQ with iQ SYBR Green Supermix (Bio-Rad). The primers used were *KRT1* (5′-GCCCTGGACATGGAGATTGCCACA-3′, 5′-TCTGGCTGGTGCTCACCGACAC-3′), *KRT10* (5′-GGAGGGTAAAATCAAGGAGTGGTA-3′, 5′-TCAATCTGCAGCAGCACGTT-3′), *Hes1* (5′-GCCAATTTGCCTTTCTCATC-3′, 5′-AGGTGACACTGCGTTAGG-3′), *Hes5* (5′-CCTGAAACACAGCAAAGCCTTC-3′, 5′-GTCAGGAACTGTACCGCCTC-3′), *Hey1* (5′-TGAATCCAGATGACCAGCTACTGT-3′, 5′-TACTTTCAGACTCCGATCGCTTAC-3′), *Hey2* (5′-GATTCCGAGAGTGCTTGAC-3′, 5′-ACAGGTGCTGAGATGAGAG-3′), *TFAM* (5′-CCAAAAAGACCTCGTTCAGC-3′, 5′-ATGTCTCCGGATCGTTTCAC-3′), *Axin2* (5′-ACCTCAAGTGCAAACTCTCACCCA-3′, 5′-AGCTGTTTCCGTGGATCTCACACT-3′), and *mRPL19* (5′-GAAGGTCAAAGGGAATGTGTTCAA-3′, 5′-TTTCGTGCTTCCTTGGTCTTAGA-3′).

Metabolic labeling

Dulbecco's modified Eagle's medium lacking both glucose and glutamine (Sigma) was prepared and supplemented with uridine (100 μg/ml) and 1mMsodiumpyruvate. Labeling medium included either 15 mM uniformly labeled D-[^{13}C]glucose and 2 mM glutamine or 25 mM glucose and 2 mM L-[^{13}C]glutamine. Primary mouse keratinocytes were grown to 80% confluence on 60-mm dishes, washed with phosphate-buffered saline (PBS), and labeled with labeling medium for 6 hours. Cells were washed two times in cold PBS and lysed in 500 μl of 50% MeOH. Metabolites were extracted by freeze-thawing three times in liquid nitrogen, and debris was removed by centrifugation. Mass spectrometry was performed as previously described (27).

ROS detection

For peroxide measurements, primary mouse keratinocytes were incubated with 2 μM 5,6-chloromethyl-2′,7′-dichlorodihydrofluorescein diacetate, acetyl ester (CM-H_2DCFDA, Invitrogen) for 1 hour. Images were taken with a Nikon BioStation CT. Fluorescence intensities were quantified with MetaMorph software. Values represent the average of 150 areas per experiment.

For superoxide measurements, primary mouse keratinocytes were incubated with 10 μM hydroethidine for 1 hour. HPLC analysis of hydroethidine oxidation products was performed as previously described (56).

Epidermal barrier assay

Excised dorsal epidermal tissue was fixed in 4% paraformaldehyde, followed by dehydration and rehydration through graded methanol. Skin was placed dermal side down in a Petri dish, and petroleum jelly was used to seal the edges of the tissue, leaving only the epidermis exposed. Tissue was stained with 1% toluidine blue for 2 min and washed with PBS.

Statistical analysis

All graphs represent the means of at least three independent biological replicates. Statistical analysis of differences between two groups was tested by unpaired, two-tailed Student's *t* test. In cases where multiple comparisons were made, one-way analysis of variance (ANOVA) was used. Bonferroni's or Dunnett's posttests were used where appropriate.

Supplementary Material

Refer to Web version on PubMed Central for supplementary material.

Acknowledgments

We are grateful to L. Liaw (Maine Medical Center Research) for the adenovirus encoding NOTCH1 ICD; J. Zielonka, J. Joseph, and B. Kalyanaraman (Medical College of Wisconsin) for invaluable help in measuring ROS concentrations and for the MVE reagent; and G. Shadel for the mouse TFAM antibody. Primary epidermal keratinocyte cultures and organotypic raft cultures were obtained from the Northwestern University Skin Disease Research Center (NU-SDRC) Keratinocyte Core Facility; lentiviral constructs were obtained from the NU-SDRC RNA/DNA Delivery Core Facility; and the NU-SDRC Pathology Core facility assisted in morphological analyses with support from the National Institute of Arthritis and Musculoskeletal and Skin Diseases of the NIH under Award Number AR057216. **Funding:** This research was also supported by NIH grants EY 06769, EY017536, and EY019463 (R.M.L.), 1F32HL099007-01 (R.B.H.), and 5R21AR061174-02 (N.S.C.) and a Dermatology Foundation Career Development Award (S.G.).

REFERENCES AND NOTES

1. Blanpain C, Fuchs E. Epidermal homeostasis: A balancing act of stem cells in the skin. Nat. Rev. Mol. Cell Biol. 2009; 10:207–217. [PubMed: 19209183]
2. Blanpain C, Fuchs E. Epidermal stem cells of the skin. Annu. Rev. Cell Dev. Biol. 2006; 22:339–373. [PubMed: 16824012]
3. Senoo M, Pinto F, Crum CP, McKeon F. p63 is essential for the proliferative potential of stem cells in stratified epithelia. Cell. 2007; 129:523–536. [PubMed: 17482546]

4. Wang X, Pasolli HA, Williams T, Fuchs E. AP-2 factors act in concert with Notch to orchestrate terminal differentiation in skin epidermis. J. Cell Biol. 2008; 183:37–48. [PubMed: 18824566]
5. Blanpain C, Lowry WE, Pasolli HA, Fuchs E. Canonical notch signaling functions as a commitment switch in the epidermal lineage. Genes Dev. 2006; 20:3022–3035. [PubMed: 17079689]
6. Alonso L, Fuchs E. The hair cycle. J. Cell Sci. 2006; 119:391–393. [PubMed: 16443746]
7. Hsu YC, Pasolli HA, Fuchs E. Dynamics between stem cells, niche, and progeny in the hair follicle. Cell. 2011; 144:92–105. [PubMed: 21215372]
8. Fuchs E. The tortoise and the hair: Slow-cycling cells in the stem cell race. Cell. 2009; 137:811–819. [PubMed: 19490891]
9. Balaban RS, Nemoto S, Finkel T. Mitochondria, oxidants, and aging. Cell. 2005; 120:483–495. [PubMed: 15734681]
10. Hamanaka RB, Chandel NS. Mitochondrial reactive oxygen species regulate cellular signaling and dictate biological outcomes. Trends Biochem. Sci. 2010; 35:505–513. [PubMed: 20430626]
11. Finkel T. Signal transduction by reactive oxygen species. J. Cell Biol. 2011; 194:7–15. [PubMed: 21746850]
12. Oeckinghaus A, Hayden MS, Ghosh S. Crosstalk in NF-κB signaling pathways. Nat. Immunol. 2011; 12:695–708. [PubMed: 21772278]
13. Zhou R, Yazdi AS, Menu P, Tschopp J. A role for mitochondria in NLRP3 inflammasome activation. Nature. 2011; 469:221–225. [PubMed: 21124315]
14. Kil IS, Lee SK, Ryu KW, Woo HA, Hu MC, Bae SH, Rhee SG. Feedback control of adrenal steroidogenesis via H_2O_2-dependent, reversible inactivation of peroxiredoxin III in mitochondria. Mol. Cell. 2012; 46:584–594. [PubMed: 22681886]
15. Tormos KV, Anso E, Hamanaka RB, Eisenbart J, Joseph J, Kalyanaraman B, Chandel NS. Mitochondrial complex III ROS regulate adipocyte differentiation. Cell Metab. 2011; 14:537–544. [PubMed: 21982713]
16. Tothova Z, Kollipara R, Huntly BJ, Lee BH, Castrillon DH, Cullen DE, McDowell EP, Lazo-Kallanian S, Williams IR, Sears C, Armstrong SA, Passegué E, DePinho RA, Gilliland DG. FoxOs are critical mediators of hematopoietic stem cell resistance to physiologic oxidative stress. Cell. 2007; 128:325–339. [PubMed: 17254970]
17. Ito K, Hirao A, Arai F, Takubo K, Matsuoka S, Miyamoto K, Ohmura M, Naka K, Hosokawa K, Ikeda Y, Suda T. Reactive oxygen species act through p38 MAPK to limit the lifespan of hematopoietic stem cells. Nat. Med. 2006; 12:446–451. [PubMed: 16565722]
18. Owusu-Ansah E, Banerjee U. Reactive oxygen species prime *Drosophila* haematopoietic progenitors for differentiation. Nature. 2009; 461:537–541. [PubMed: 19727075]
19. Smith J, Ladi E, Mayer-Proschel M, Noble M. Redox state is a central modulator of the balance between self-renewal and differentiation in a dividing glial precursor cell. Proc. Natl. Acad. Sci. U.S.A. 2000; 97:10032–10037. [PubMed: 10944195]
20. Tsatmali M, Walcott EC, Crossin KL. Newborn neurons acquire high levels of reactive oxygen species and increased mitochondrial proteins upon differentiation from progenitors. Brain Res. 2005; 1040:137–150. [PubMed: 15804435]
21. Diehn M, Cho RW, Lobo NA, Kalisky T, Dorie MJ, Kulp AN, Qian D, Lam JS, Ailles LE, Wong M, Joshua B, Kaplan MJ, Wapnir I, Dirbas FM, Somlo G, Garberoglio C, Paz B, Shen J, Lau SK, Quake SR, Brown JM, Weissman IL, Clarke MF. Association of reactive oxygen species levels and radioresistance in cancer stem cells. Nature. 2009; 458:780–783. [PubMed: 19194462]
22. Chen CT, Shih YR, Kuo TK, Lee OK, Wei YH. Coordinated changes of mitochondrial biogenesis and antioxidant enzymes during osteogenic differentiation of human mesenchymal stem cells. Stem Cells. 2008; 26:960–968. [PubMed: 18218821]
23. Campbell CT, Kolesar JE, Kaufman BA. Mitochondrial transcription factor A regulates mitochondrial transcription initiation, DNA packaging, and genome copy number. Biochim. Biophys. Acta. 2012; 1819:921–929. [PubMed: 22465614]
24. Weinberg F, Hamanaka R, Wheaton WW, Weinberg S, Joseph J, Lopez M, Kalyanaraman B, Mutlu GM, Budinger GR, Chandel NS. Mitochondrial metabolism and ROS generation are essential for Kras-mediated tumorigenicity. Proc. Natl. Acad. Sci. U.S.A. 2010; 107:8788–8793. [PubMed: 20421486]

25. Larsson NG, Wang J, Wilhelmsson H, Oldfors A, Rustin P, Lewandoski M, Barsh GS, Clayton DA. Mitochondrial transcription factor A is necessary for mtDNA maintenance and embryogenesis in mice. Nat. Genet. 1998; 18:231–236. [PubMed: 9500544]
26. DeBerardinis RJ, Lum JJ, Hatzivassiliou G, Thompson CB. The biology of cancer: Metabolic reprogramming fuels cell growth and proliferation. Cell Metab. 2008; 7:11–20. [PubMed: 18177721]
27. Mullen AR, Wheaton WW, Jin ES, Chen PH, Sullivan LB, Cheng T, Yang Y, Linehan WM, Chandel NS, DeBerardinis RJ. Reductive carboxylation supports growth in tumour cells with defective mitochondria. Nature. 2012; 481:385–388. [PubMed: 22101431]
28. Hennings H, Michael D, Cheng C, Steinert P, Holbrook K, Yuspa SH. Calcium regulation of growth and differentiation of mouse epidermal cells in culture. Cell. 1980; 19:245–254. [PubMed: 6153576]
29. Wang Y, DuBois JL, Hedman B, Hodgson KO, Stack TD. Catalytic galactose oxidasemodels: Biomimetic Cu(II)-phenoxyl-radical reactivity. Science. 1998; 279:537–540. [PubMed: 9438841]
30. Echtay KS, Murphy MP, Smith RA, Talbot DA, Brand MD. Superoxide activates mitochondrial uncoupling protein 2 from the matrix side. Studies using targeted antioxidants. J. Biol. Chem. 2002; 277:47129–47135. [PubMed: 12372827]
31. Baker K, Marcus CB, Huffman K, Kruk H, Malfroy B, Doctrow SR. Synthetic combined superoxide dismutase/catalase mimetics are protective as a delayed treatment in a rat stroke model: A key role for reactive oxygen species in ischemic brain injury. J. Pharmacol. Exp. Ther. 1998; 284:215–221. [PubMed: 9435181]
32. Matlib MA, Zhou Z, Knight S, Ahmed S, Choi KM, Krause-Bauer J, Phillips R, Altschuld R, Katsube Y, Sperelakis N, Bers DM. Oxygen-bridged dinuclear ruthenium amine complex specifically inhibits Ca^{2+} uptake into mitochondria in vitro and in situ in single cardiac myocytes. J. Biol. Chem. 1998; 273:10223–10231. [PubMed: 9553073]
33. Gangatirkar P, Paquet-Fifield S, Li A, Rossi R, Kaur P. Establishment of 3D organotypic cultures using human neonatal epidermal cells. Nat. Protoc. 2007; 2:178–186. [PubMed: 17401352]
34. Moriyama M, Durham AD, Moriyama H, Hasegawa K, Nishikawa S, Radtke F, Osawa M. Multiple roles of Notch signaling in the regulation of epidermal development. Dev. Cell. 2008; 14:594–604. [PubMed: 18410734]
35. Rangarajan A, Talora C, Okuyama R, Nicolas M, Mammucari C, Oh H, Aster JC, Krishna S, Metzger D, Chambon P, Miele L, Aguet M, Radtke F, Dotto GP. Notch signaling is a direct determinant of keratinocyte growth arrest and entry into differentiation. EMBO J. 2001; 20:3427–3436. [PubMed: 11432830]
36. Huelsken J, Vogel R, Erdmann B, Cotsarelis G, Birchmeier W. β-Catenin controls hair follicle morphogenesis and stem cell differentiation in the skin. Cell. 2001; 105:533–545. [PubMed: 11371349]
37. Gat U, DasGupta R, Degenstein L, Fuchs E. De novo hair follicle morphogenesis and hair tumors in mice expressing a truncated β-catenin in skin. Cell. 1998; 95:605–614. [PubMed: 9845363]
38. Funato Y, Michiue T, Asashima M, Miki H. The thioredoxin-related redox-regulating protein nucleoredoxin inhibits Wnt–β-catenin signalling through dishevelled. Nat. Cell Biol. 2006; 8:501–508. [PubMed: 16604061]
39. Metallo CM, Gameiro PA, Bell EL, Mattaini KR, Yang J, Hiller K, Jewell CM, Johnson ZR, Irvine DJ, Guarente L, Kelleher JK, Vander Heiden MG, Iliopoulos O, Stephanopoulos G. Reductive glutamine metabolism by IDH1 mediates lipogenesis under hypoxia. Nature. 2012; 481:380–384. [PubMed: 22101433]
40. Wise DR, Ward PS, Shay JE, Cross JR, Gruber JJ, Sachdeva UM, Platt JM, DeMatteo RG, Simon MC, Thompson CB. Hypoxia promotes isocitrate dehydrogenase-dependent carboxylation of α-ketoglutarate to citrate to support cell growth and viability. Proc. Natl. Acad. Sci. U.S.A. 2011; 108:19611–19616. [PubMed: 22106302]
41. Peng H, Kaplan N, Hamanaka RB, Katsnelson J, Blatt H, Yang W, Hao L, Bryar PJ, Johnson RS, Getsios S, Chandel NS, Lavker RM. microRNA-31/factor-inhibiting hypoxia-inducible factor 1 nexus regulates keratinocyte differentiation. Proc. Natl. Acad. Sci. U.S.A. 2012; 109:14030–14034. [PubMed: 22891326]

42. Masson N, Singleton RS, Sekirnik R, Trudgian DC, Ambrose LJ, Miranda MX, Tian YM, Kessler BM, Schofield CJ, Ratcliffe PJ. The FIH hydroxylase is a cellular peroxide sensor that modulates HIF transcriptional activity. EMBO Rep. 2012; 13:251–257. [PubMed: 22310300]
43. Mukherjee T, Kim WS, Mandal L, Banerjee U. Interaction between Notch and Hif-α in development and survival of Drosophila blood cells. Science. 2011; 332:1210–1213. [PubMed: 21636775]
44. Gustafsson MV, Zheng X, Pereira T, Gradin K, Jin S, Lundkvist J, Ruas JL, Poellinger L, Lendahl U, Bondesson M. Hypoxia requires notch signaling to maintain the undifferentiated cell state. Dev. Cell. 2005; 9:617–628. [PubMed: 16256737]
45. Hamanaka RB, Chandel NS. Mitochondrial reactive oxygen species regulate hypoxic signaling. Curr. Opin. Cell Biol. 2009; 21:894–899. [PubMed: 19781926]
46. Bodemer C, R[illegible]tig A, Rustin P, Cormier V, Niaudet P, Saudubray JM, Rabier D, Munnich A, de Prost Y. Hair and skin disorders as signs of mitochondrial disease. Pediatrics. 1999; 103:428–433. [PubMed: 9925836]
47. Baris OR, Klose A, Kloepper JE, Weiland D, Neuhaus JF, Schauen M, Wille A, Müller A, Merkwirth C, Langer T, Larsson NG, Krieg T, Tobin DJ, Paus R, Wiesner RJ. The mitochondrial electron transport chain is dispensable for proliferation and differentiation of epidermal progenitor cells. Stem Cells. 2011; 29:1459–1468. [PubMed: 21780252]
48. Napoli C, Martin-Padura I, de Nigris F, Giorgio M, Mansueto G, Somma P, Condorelli M, Sica G, De Rosa G, Pelicci P. Deletion of the $p66^{Shc}$ longevity gene reduces systemic and tissue oxidative stress, vascular cell apoptosis, and early atherogenesis in mice fed a high-fat diet. Proc. Natl. Acad. Sci. U.S.A. 2003; 100:2112–2116. [PubMed: 12571362]
49. Richter C, Park JW, Ames BN. Normal oxidative damage to mitochondrial and nuclear DNA is extensive. Proc. Natl. Acad. Sci. U.S.A. 1988; 85:6465–6467. [PubMed: 3413108]
50. Bjelakovic G, Nikolova D, Gluud LL, Simonetti RG, Gluud C. Mortality in randomized trials of antioxidant supplements for primary and secondary prevention: Systematic review and meta-analysis. JAMA. 2007; 297:842–857. [PubMed: 17327526]
51. Chong EW, Wong TY, Kreis AJ, Simpson JA, Guymer RH. Dietary antioxidants and primary prevention of age related macular degeneration: Systematic review and meta-analysis. BMJ. 2007; 335:755. [PubMed: 17923720]
52. Storch A, Jost WH, Vieregge P, Spiegel J, Greulich W, Durner J, Müller T, Kupsch A, Henningsen H, Oertel WH, Fuchs G, Kuhn W, Niklowitz P, Koch R, Herting B, Reichmann H. German Coenzyme Q_{10} Study Group, Randomized, double-blind, placebo-controlled trial on symptomatic effects of coenzyme Q_{10} in Parkinson disease. Arch. Neurol. 2007; 64:938–944. [PubMed: 17502459]
53. Kang JH, Cook NR, Manson JE, Buring JE, Albert CM, Grodstein F. Vitamin E, vitamin C, beta carotene, and cognitive function among women with or at risk of cardiovascular disease: The Women's Antioxidant and Cardiovascular Study. Circulation. 2009; 119:2772–2780. [PubMed: 19451353]
54. Lin J, Cook NR, Albert C, Zaharris E, Gaziano JM, Van Denburgh M, Buring JE, Manson JE. Vitamins C and E and β carotene supplementation and cancer risk: A randomized controlled trial. J. Natl. Cancer Inst. 2009; 101:14–23. [PubMed: 19116389]
55. Meyers C, Laimins LA. In vitro systems for the study and propagation of human papillomaviruses. Curr. Top. Microbiol. Immunol. 1994; 186:199–215. [PubMed: 8205842]
56. Zielonka J, Vasquez-Vivar J, Kalyanaraman B. Detection of 2-hydroxyethidium in cellular systems: A unique marker product of superoxide and hydroethidine. Nat. Protoc. 2008; 3:8–21. [PubMed: 18193017]

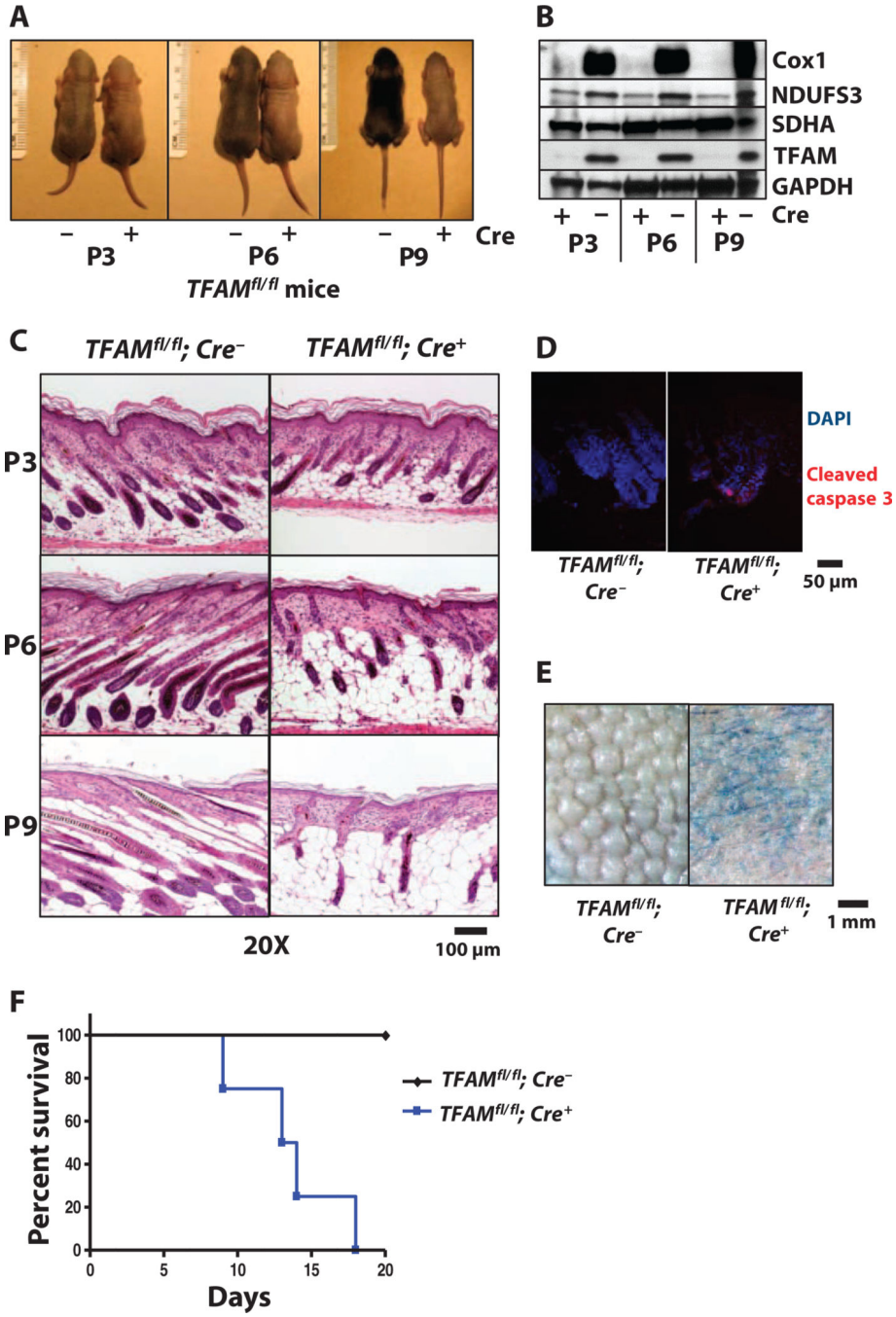

Fig. 1.

Deletion of TFAM in the epidermis results in progressive loss of hair follicles and decreased life span. (**A**) Representative images of control and *TFAM* cKO mice at P3, P6, and P9 showing lack of hair development in *TFAM* cKO mice (representative of 12 mice per genotype per day). (**B**) Western blot analysis of footpad skin lysates from control and *TFAM* cKO mice demonstrating loss of TFAM and Cox1 (which is encoded by the mitochondrial genome) protein (representative of three independent Western blots). (**C**) Images of skin sections from control and *TFAM* cKO mice stained with hematoxylin and eosin (H&E),

demonstrating progressive loss of hair follicles in *TFAM* cKO epidermis (representative of three mice per genotype per day). (**D**) Immunofluorescence staining of control and *TFAM* cKO hair follicles for cleaved caspase 3, demonstrating onset of catagen (representative of two mice per genotype). (**E**) Back skin from control and *TFAM* cKO mice (P15) stained with toluidine blue, demonstrating an epidermal barrier defect in *TFAM* cKO mice (representative of three mice per genotype). (**F**) Kaplan-Meier survival analysis of control and *TFAM* cKO mice demonstrating reduced survival of *TFAM* cKO mice (n = 12 mice per genotype).

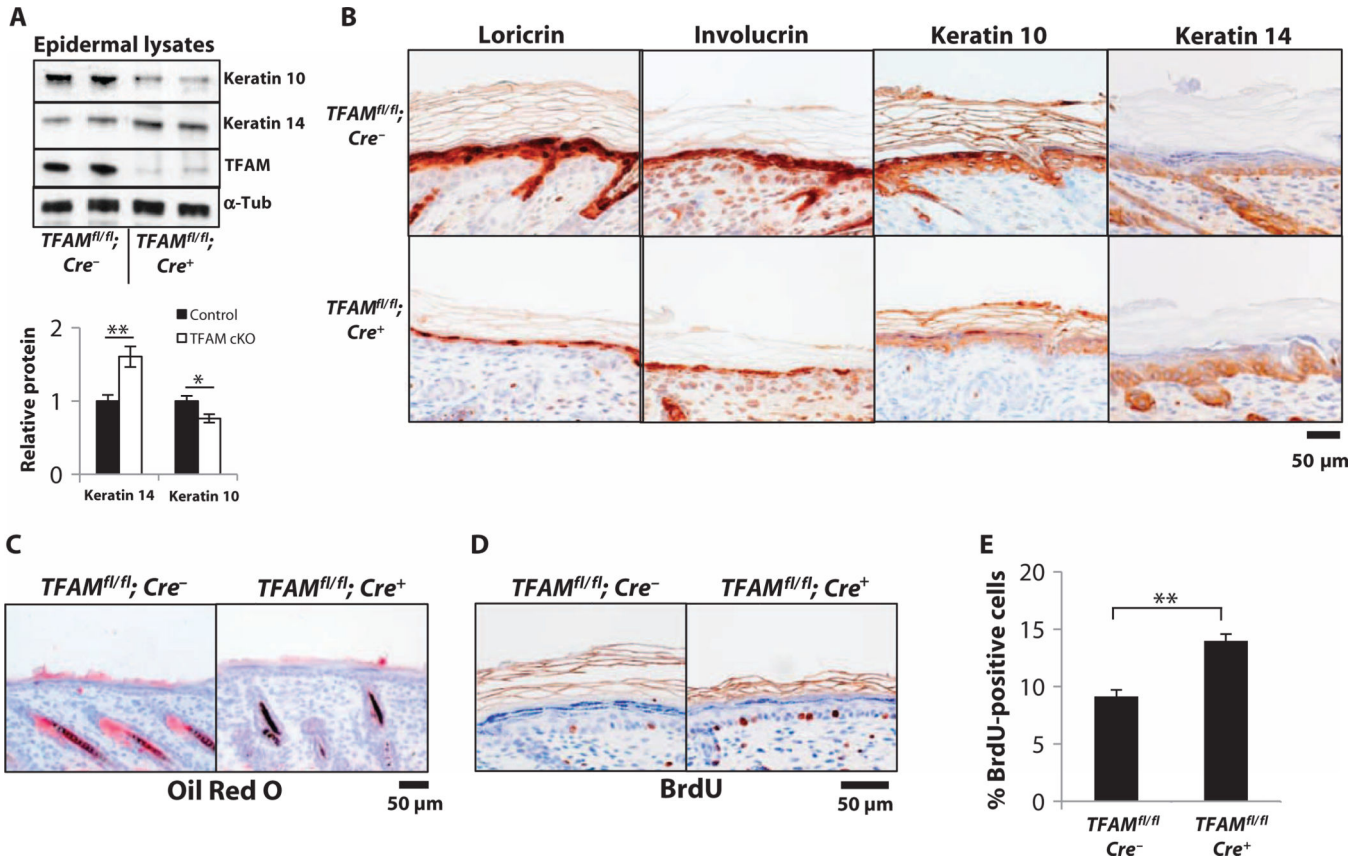

Fig. 2.

TFAM-deficient epidermis displays reduced abundance of differentiation markers and increased proliferation compared with control epidermis. (**A**) Representative Western blot analysis of epidermal lysates from control and *TFAM* cKO mice at P9. Graph represents relative normalized keratin 10 or keratin 14 protein amounts ± SEM. $n = 7$ mice per genotype. $^{*}P < 0.05$, $^{**}P < 0.01$. (**B**) Skin sections from control and *TFAM* cKO mice at P6 stained for the terminal differentiation markers loricrin, involucrin, or keratin 10 or the basal marker keratin 14 (representative of two mice per genotype). (**C**) Control and *TFAM* cKO back skin stained with Oil Red O, demonstrating a loss of sebaceous glands (representative of two mice per genotype). (**D**) Skin sections from control and *TFAM* cKO mice at P6, taken after a BrdU pulse, were stained for BrdU incorporation to determine epidermal proliferation rates (representative of three mice per genotype). (**E**) Quantification of epidermal proliferation rates as assessed by percentage of epidermal basal cells per skin section that stained positive for BrdU incorporation. Graph shows means ± SEM. $n = 3$ mice per genotype. $^{**}P < 0.01$.

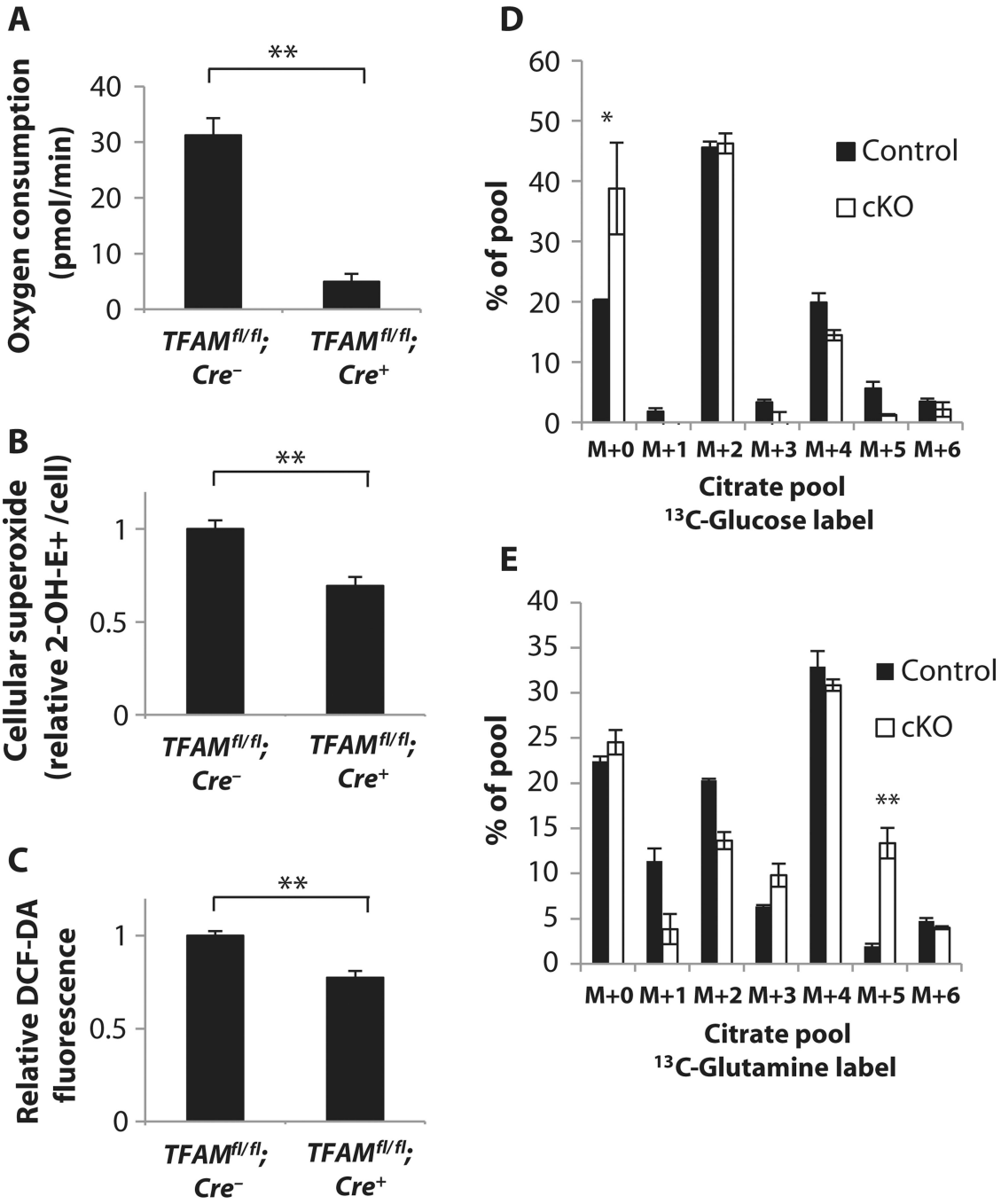

Fig. 3.

Altered cellular metabolism and ROS concentrations in *TFAM* cKO primary keratinocytes. (**A**) Oxygen consumption rates of control and *TFAM* cKO keratinocytes. Graph shows means ± SEM. $n = 8$ independent keratinocyte pools. $^{**}P < 0.01$. (**B**) Cellular superoxide concentrations. Control and *TFAM* cKO keratinocytes were treated with hydroethidine, and concentrations of its oxidation product 2-hydroxyethidium (2-OH-E+) were measured by high-performance liquid chromatography (HPLC). Graph shows means relative to control ± SEM. $n = 5$ independent keratinocyte pools. $^{**}P < 0.01$. (**C**) Cellular H_2O_2 concentrations

measured by DCF-DA fluorescence. Graph shows means relative to control ± SEM. $n = 4$ independent keratinocyte pools. $^{**}P < 0.01$. (**D** and **E**) Primary keratinocytes from control or *TFAM* cKO mice were labeled with either [^{13}C]glucose (D) or [^{13}C]glutamine (E). ^{13}C enrichment in cellular citrate pools was analyzed by mass spectrometry. Graph shows means ± SD. $n = 3$ independent keratinocyte pools. $^{**}P < 0.01$.

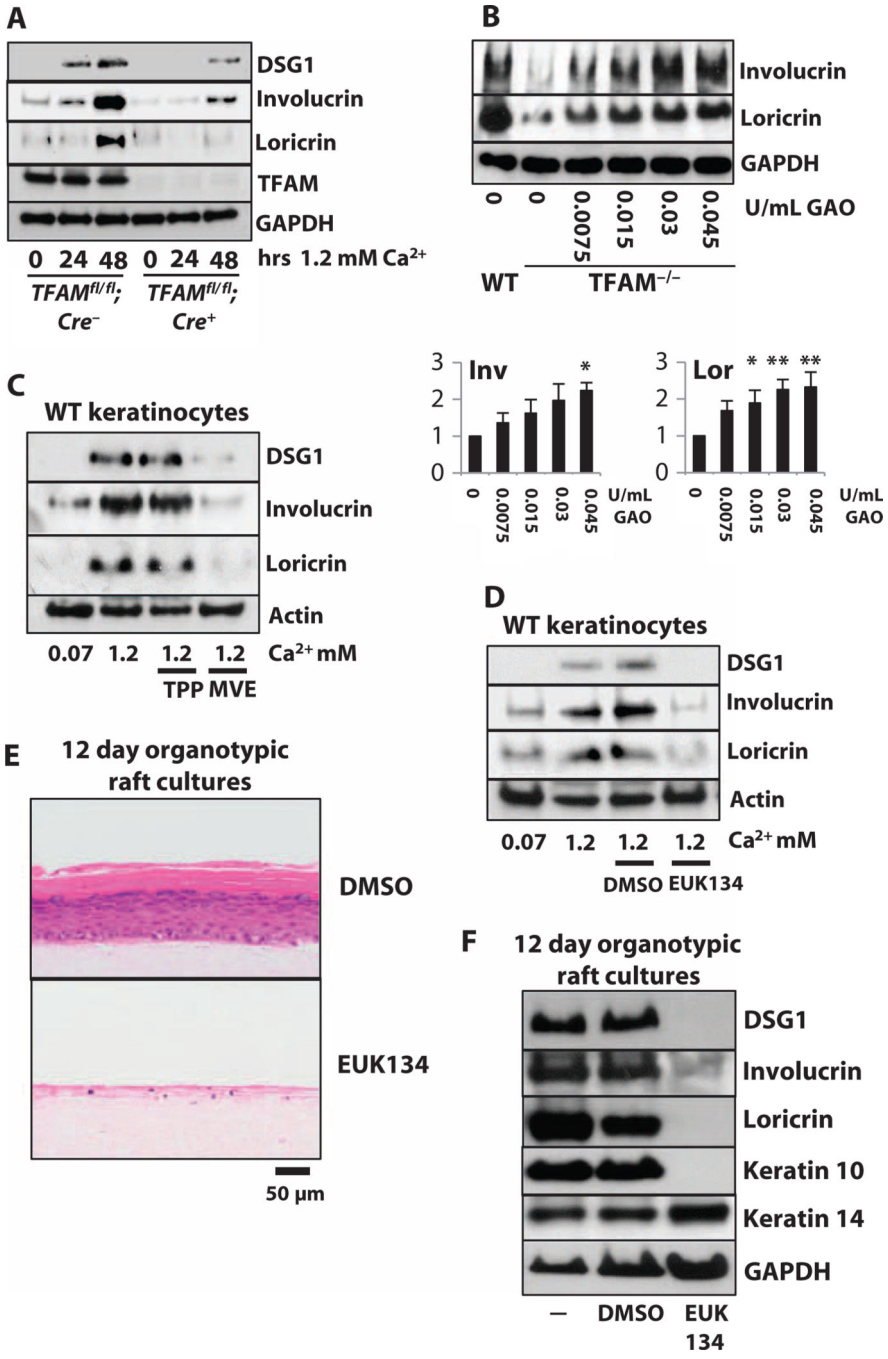

Fig. 4.

Primary epidermal keratinocytes from *TFAM* cKO mice display impaired differentiation in vitro. (**A**) Western blot analysis of cellular lysates from untreated or $CaCl_2$-treated control and *TFAM* cKO mouse keratinocytes (representative of three independent experiments). (**B**) Western blot analysis of cellular lysates from control and *TFAM* cKO mouse keratinocytes treated with $CaCl_2$ and galactose. *TFAM* cKO keratinocytes were treated with the indicated amounts of galactose oxidase (GAO) (representative of three independent experiments). Graphs represent mean fold protein induction over GAO (0 U/ml) ± SEM. **P* < 0.05, ***P* <

0.01. (**C**) Western blot analysis of cellular lysates from control keratinocytes left untreated or treated with $CaCl_2$ in the presence or absence of TPP or MVE (representative of three independent experiments). (**D**) Western blot analysis of cellular lysates from control keratinocytes left untreated or treated with $CaCl_2$ in the presence of either EUK134 or dimethyl sulfoxide (DMSO) as vehicle control (representative of three independent experiments. (**E**) H&E-stained sections taken from 12-day human organotypic keratinocyte raft cultures treated with DMSO or EUK134 from day 0 (representative of two independent experiments). (**F**) Western blot analysis of differentiation markers in human organotypic keratinocyte raft cultures (representative of two independent experiments).

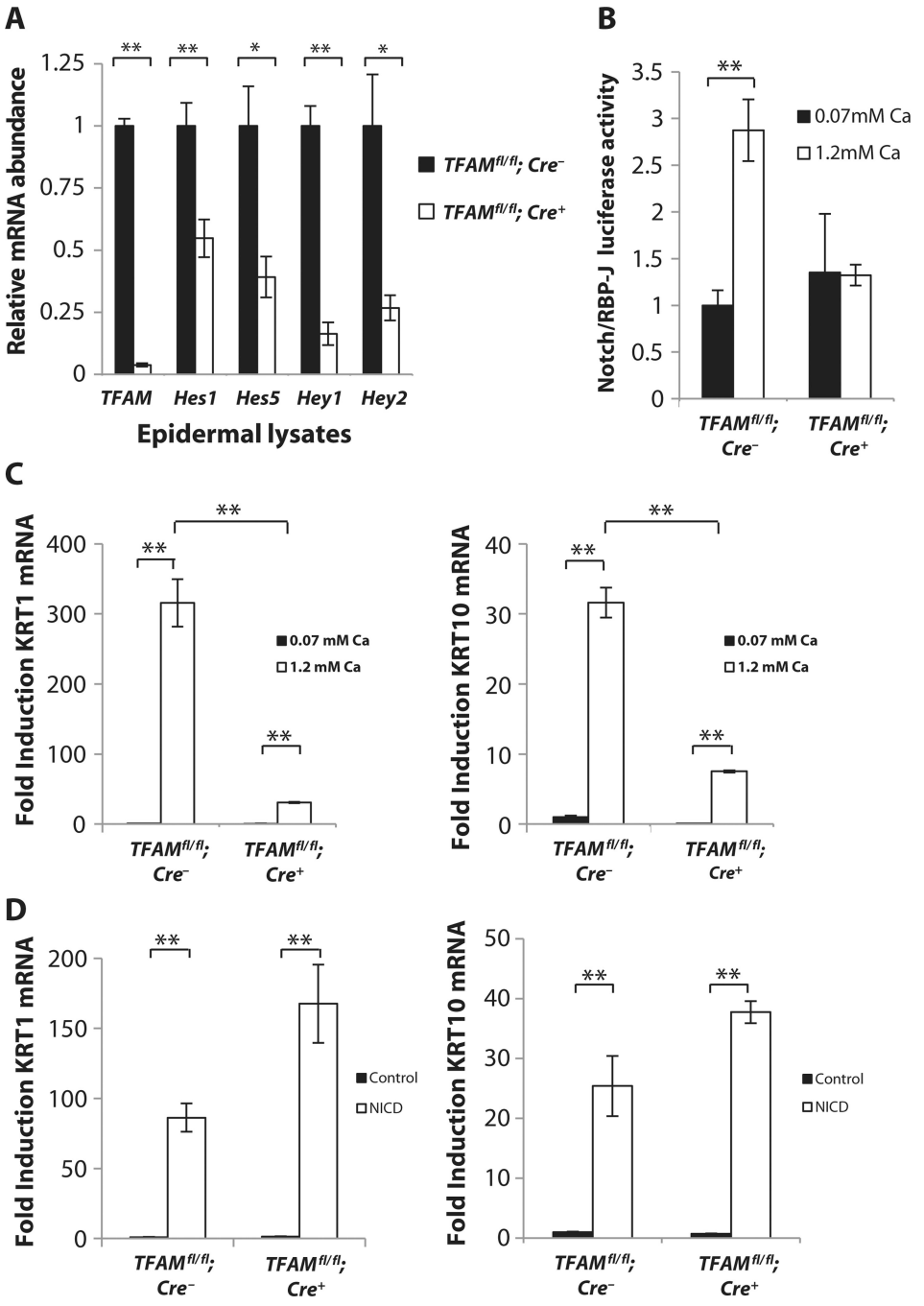

Fig. 5.

Mitochondrial ROS are required for transduction of Notch signals during keratinocyte differentiation. (**A**) Quantitative reverse transcription polymerase chain reaction (qRT-PCR) analysis of epidermal lysates from control and *TFAM* cKO mice at P9, demonstrating reduced expression of Notch target mRNAs. Graph shows means relative to control mRNA expression ± SEM. $n = 4$ mice per genotype. *$P < 0.05$, **$P < 0.01$. (**B**) Notch/RBP-J luciferase reporter activity in lysates of control and *TFAM* cKO keratinocytes treated with $CaCl_2$ for 0 or 48 hours. Graph shows means relative to control undifferentiated ± SEM. n =

3 independent keratinocyte pools. ***P* < 0.01. (**C**) qRT-PCR analysis of *keratin 1* or *keratin 10* mRNA abundance in control and *TFAM* cKO keratinocytes cultured at the indicated $CaCl_2$ concentrations. Graphs show means relative to control undifferentiated ± SEM. *n* = 3 independent keratinocyte pools. ***P*<0.01. (**D**) qRT-PCR analysis of *keratin 1* or *keratin 10* mRNA abundance in control or *TFAM* cKO keratinocytes after infection with adenovirus encoding GFP (control) or adenovirus encoding the NICD. Graphs show means relative to control cells with control infection ± SEM. *n* = 3 independent keratinocyte pools. ***P* < 0.01.

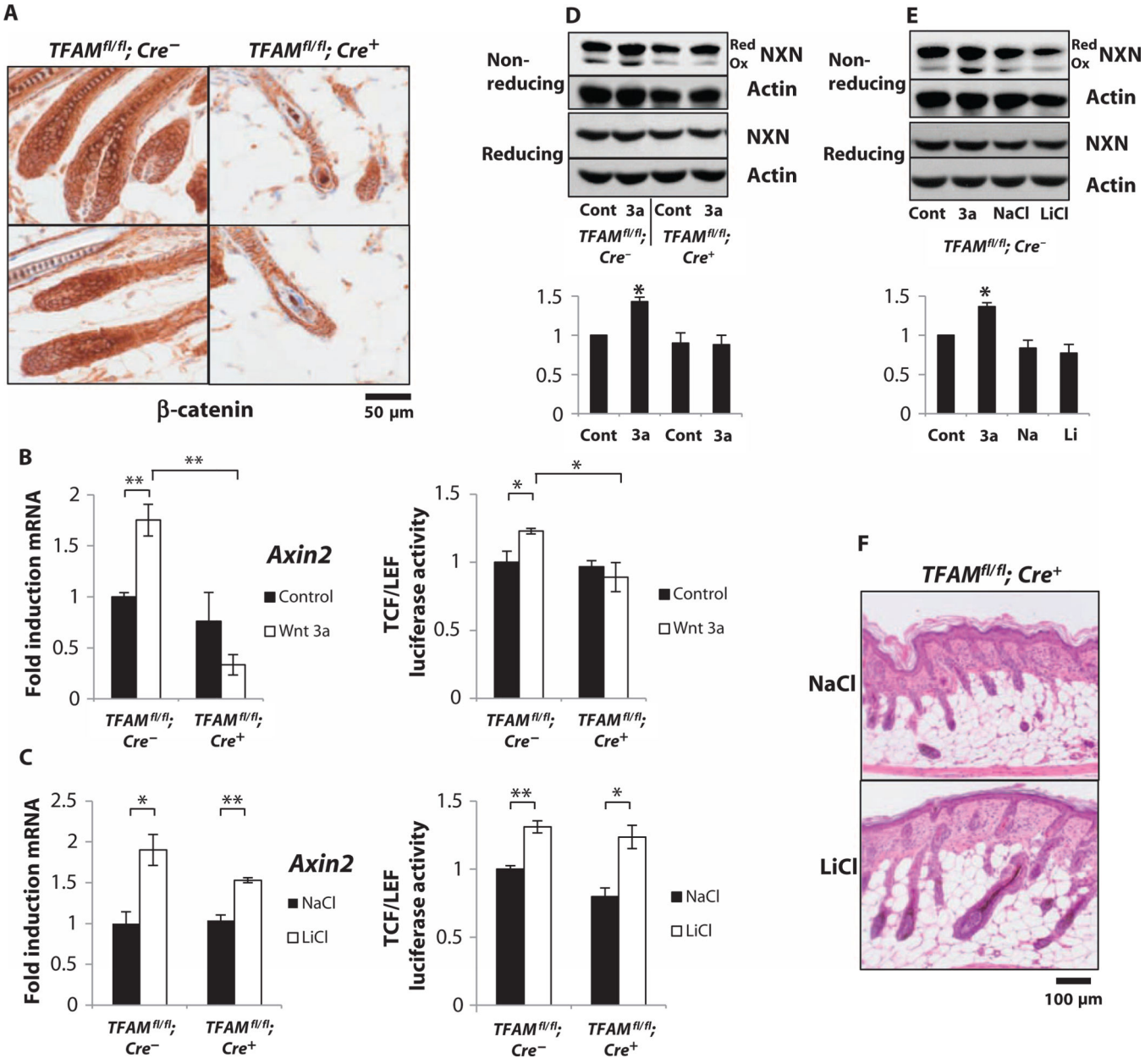

Fig. 6.

Mitochondrial ROS generation is required for β-catenin activation in the epidermis. (**A**) Skin sections from control and *TFAM* cKO mice at P6 stained for β-catenin (representative of two mice per genotype). (**B**) Fold induction of *Axin2* mRNA or TCF/LEF luciferase reporter in control or *TFAM* cKO keratinocytes after treatment with Wnt3a or control treatment. For qRT-PCR experiments, control or Wnt3a-conditioned medium was used for treatment. For luciferase experiments, adenoviral infection with either Wnt3a or GFP (control)–encoding virus was used. Graphs show means relative to control cells with control treatment ± SEM. *n* = 3 independent keratinocyte pools. **P* ≤ 0.05, ***P* < 0.01. (**C**) Fold induction of *Axin2* mRNA or TCF/LEF luciferase reporter in control or TFAM cKO keratinocytes after treatment with LiCl or NaCl as control. Graphs show means relative to control cells with

NaCl treatment ± SEM. $n = 3$ independent keratinocyte pools. *$P < 0.05$, **$P < 0.01$. (**D** and **E**) Nonreducing or reducing Western blot analysis of (D) control or *TFAM* cKO keratinocytes infected with adenovirus encoding either Wnt3a or GFP as control or (E) control keratinocytes treated with NaCl or LiCl. Oxidized and reduced forms of NXN are indicated on nonreducing blots. Graphs represent fold increase in oxidized NXN relative to fold increase in reduced NXN and show the means of three experiments ± SEM. *$P < 0.05$. (**F**) Back skin sections from P7 *TFAM* cKO mice stained with H&E. Mothers of litters received daily injections of either LiCl or NaCl beginning at P0 (representative of four mice per treatment).